Supplementary Information

Impact of Hydrogen Bonding Interactions on Graft−Matrix Wetting and Structure in Polymer Nanocomposites

Arjita Kulshreshtha [1], Kevin J. Modica [1]and Arthi Jayaraman [1,2,*]

1. Department of Chemical and Biomolecular Engineering, 150 Academy St, Colburn Laboratory, University of Delaware, Newark DE 19716

2. Department of Materials Science and Engineering, 201 Dupont Hall, University of Delaware, Newark DE 19716

* corresponding author arthij@udel.edu

I. Additional details of the model.

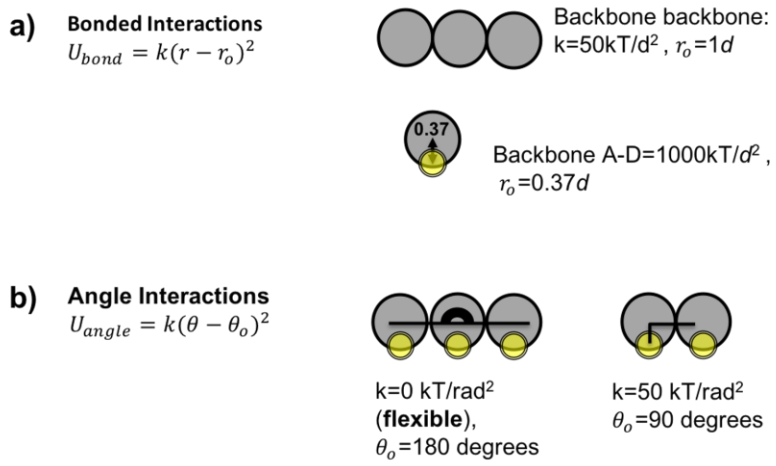

Figure S1. *Schematic showing a) bonded potential parameters between backbone-backbone beads and backbone A-D beads b) angle potential parameters between consecutive backbone beads and A-D sites and backbone chains.*

The main paper method section describes the key features of the model used in this work. Here we provide some additional details, and relevant equations for various parts of the model described in the main paper.

The graft and matrix beads are linked through harmonic bonds (Figure S1a) of the form given by

$$U_{bond} = k_{bond}(r - r_o)^2, \quad (1)$$

where *r* is the distance between the centers of interacting beads, $k_{bond} = 50kT/d^2$ is the harmonic bond force constant where *k* is Boltzmann constant and *kT* corresponds to thermal energy, and $r_o = 1d$ is the equilibrium bond distance. Harmonic bonds with parameters discussed above are also used to tether the graft chains to the grafting site beads of the nanoparticle.

To tune graft and matrix flexibility, we use harmonic angle potentials between three consecutive beads in either the graft or the matrix chains (Figure S1b) given by

$$U_{angle} = k_{angle}(\theta - \theta_o)^2 , \quad (2)$$

where θ is the bond angle between three consecutive beads in either the graft or the matrix chain. For this study described in the main paper we focus on fully flexible polymer chains and therefore, maintain $k_{angle} = 0$ *kT/rad*^{2} and $\theta_o = \pi$ radians .

To act as hydrogen bonding sites, we introduce acceptor sites (A) on grafted chain beads and donor sites (D) on matrix chain beads(see main paper Figure 1). As done in our previous studies[1], these acceptor donor (A/D) sites are modeled as spheres of size 0.3*d*. A/D sites are bonded to graft and matrix beads by harmonic bonds (Figure S1a) of force constant $k_{bond} = 1000kT/d^2$ and equilibrium bond distance $r_o = 0.37d$. Harmonic angle potentials (Figure S1b) between an acceptor or donor bead and two adjacent

graft/matrix monomer beads with $k_{angle} = 50\ kT/rad^2$ and $\theta_o = \pi/2$ radians maintain the A or D sites at right angles to their parent graft or matrix beads. We exclude angle potential interactions for acceptor and donor sites at the last bead of graft and matrix chains to allow them to explore all angular conformations thereby preserving end effects.

Non-bonded interactions between graft-graft (GG) and matrix-matrix (MM) bead pairs are modeled using Lennard Jones (LJ)[2] potential given by

$$U_x(r) = 4\varepsilon_x\left[(\frac{\sigma_x}{r})^{12} - (\frac{\sigma_x}{r})^{6}\right] + 4\varepsilon_x\left[(\frac{\sigma_x}{r_{cut}})^{12} - (\frac{\sigma_x}{r_{cut}})^{6}\right]\ ;\ r < r_{cut} \quad (3)$$

and $U_x(r)$ is zero otherwise. Here *x* represents either graft-graft (GG) or matrix-matrix (MM) interaction with the parameters $\varepsilon_{GG} = \varepsilon_{MM} = 0.5kT$, $\sigma_{GG} = \sigma_{MM} = 1d$ and $r_{cut} = 2d$.

Non-bonded interactions between graft and matrix (GM) pairs (Figure S2a) are modeled using LJ potential with σ_{GM} = 1.0d and $r_{cut} = 2.0d$ and varying ε_{GM} to achieve a desired graft-matrix Flory Huggins interaction parameter χ_{GM} (scaled by lattice coordination number z) defined as

$$\chi_{GM} = \frac{\chi^*_{GM}}{z} = \frac{-\varepsilon_{GM} - 0.5(-\varepsilon_{GG} - \varepsilon_{MM})}{k_B T}, \quad (4)$$

In some cases, graft and matrix chain beads are modeled to have purely repulsive interactions using the Weeks Chandler Andersen (WCA)[3] potential for GG, MM and GM interactions given as

$$U_x(r) = 4\varepsilon_x\left[(\frac{\sigma_x}{r})^{12} - (\frac{\sigma_x}{r})^{6}\right] + 4\varepsilon_x\left[(\frac{\sigma_x}{r_{cut}})^{12} - (\frac{\sigma_x}{r_{cut}})^{6}\right];\ r < r_{cut} \quad (5)$$

and $U_x(r)$ is zero otherwise. Here *x* is either GG, MM or GM and $r_{cut} = 1.1225d$.
Similarly, in some cases, acceptor and donor beads are modeled to have purely repulsive interactions using WCA potentials as shown in equation 5.

The non-bonded A-D interaction is defined using LJ potential with $\sigma_{AD} = 0.3d$, $r_{cut} = 2\sigma_{AD}$, and $\varepsilon_{AD} = 13kT$ to mimic the maximum strength of OH:N h-bonded pair. We selected this specific chemistry of donor and acceptor based on work by Hayward and coworkers[4]. The strength of A-D attraction (i.e., value of ε_{AD}) can be varied to mimic varying h-bonding donor-acceptor pair chemistry.

The maximum hydrogen bond energy for a OH:N interaction pair is approximately 29 kJ/mole for ammonia – water hydrogen bonding interaction[5]. If the reduced temperature of T* = 1 in simulated systems corresponds to T = 298K, then based on

$$T^* = \frac{k_B T}{\varepsilon^*} \quad (6)$$

we get the energy scale from simulations to be $\varepsilon^* = 2.214$ kJ/mole. Hence, we choose the strength of A-D interaction in our simulations to be $\varepsilon_{AD} \sim 13kT$ to approximate the hydrogen bond energy of OH:N interactions.

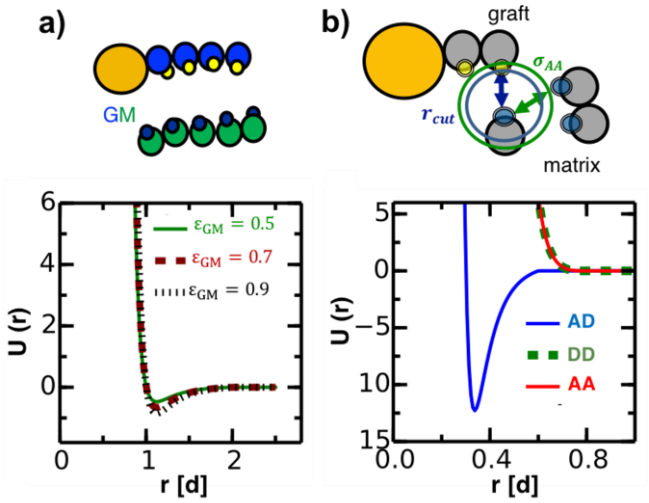

Figure S2. *a) Graft-matrix (GM) interaction potential as a function of distance r between centers of interacting G and M beads for varying strengths of* ε_{GM}. *b) Directional and specific hydrogen bonding interaction is achieved via bonded interactions described in the text and nonbonded interactions including an attractive interaction potential between A-D sites (blue line) and a repulsive potential between like A-A (red line) and D-D (green dashed line); the like A-A and D-D repulsive interaction preserves the specificity of A-D interaction and does not allow formation of A-D-A or D-A-D attractive interactions.*

II. Additional Results

A. Proof that the chosen volume fraction η of 0.367 represents melt-like conditions

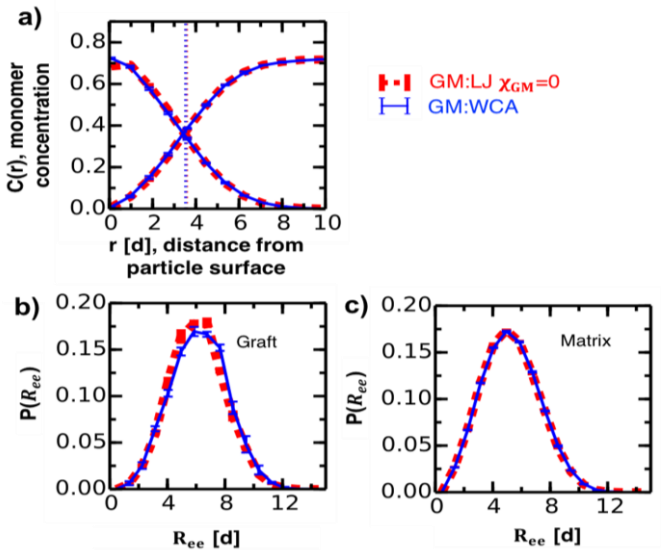

Figure S3*. a) Graft and matrix monomer concentration profiles for PNCs with repulsive A-D interaction and graft-matrix interaction specified by LJ potential with $\chi_{GM} = 0$ (red dashed line) and purely repulsive WCA potential (blue solid line). Probability distribution of the end-end distances, P(R_{ee}) vs R_{ee} for b) graft chains and c) matrix chains. These results are for D=5d, graft chain length N_G=20, grafting densities Σ =0.65 chains/d^2 placed within a matrix of chain length of N_M=20*

Figure S3a shows a comparison between monomer concentration profiles for PNCs with repulsive interaction between A-D sites for the case where graft-matrix interactions are defined using purely repulsive WCA potential (blue lines) and for the case where the graft-matrix interactions are defined via attractive LJ potential ($\varepsilon_{GM} = \varepsilon_{GG} = \varepsilon_{MM} = 0.5kT$) but there is no net attraction between graft and matrix chains (red dashed lines). The overlapping monomer concentration profiles and probability distribution of end-end distances of graft and matrix chains [b)-c)] for the two cases suggest that PNCs chain conformations are not sensitive to the attractive interactions, and essentially the PNC is incompressible as expected for polymers in melt like conditions.

B. Quantification of the grafted layer wetting for select PNCs

Table S1. *Average number of matrix beads within grafted layer thickness and average number of matrix chains interacting with each graft chain for parameter cases as shown*

N_G, N_M	Grafting Density (chains/d^2)	Interactions	Average number of matrix beads within grafted layer thickness (*dashed lines in concentration profiles*)	Average number of matrix chains interacting with each graft chain
20, 20	0.65	χ_{GM} = -0.4 Repulsive AD interaction	1595.20 ± 12.48	31.00 ± 1.45
20, 20	0.65	χ_{GM} = -0.5 Repulsive AD interaction	1734.02 ± 6.40	32.77 ± 0.13
20, 20	0.65	χ_{GM} = 0 Attractive AD interaction	1728.80 ± 46.23	12.40 ± 0.63

20, 20	0.32	χ_{GM} = -0.4 Repulsive AD interaction	1526.30 ± 2.78	25.52 ± 0.16
20, 20	0.32	χ_{GM} = 0 Attractive AD interaction	1614.30 ± 1.25	11.39 ± 0.16
20, 60	0.65	χ_{GM} = -0.5 Repulsive AD interaction	1724.02 ± 15.13	27.50 ± 1.50
20, 60	0.65	χ_{GM} = 0 Attractive AD interaction	1714.32 ± 41.62	11.60 ± 0.60

C. Impact of strength of hydrogen bonding interaction on wetting behavior

Even though we present results for 13*kT* in the main paper, we also explored other A-D interaction strengths. Figure S4 shows the impact of the A-D interaction strength on the extent of wetting as well as the graft chain conformations. As the A-D interaction becomes increasingly attractive from 4*kT* to 13*kT*, the grafted layer wetting by matrix chains increases and grafted layer extends, as expected. Interestingly, the data in Figure S4 shows that PNC chemistries with h-bonding strength of 8*kT* and 13*kT* will likely result in similar wetting and chain conformations. This suggests that the grafted layer wetting reaches a saturation limit beyond which any additional hydrogen bonding interaction strength will lead to minimal increase in grafted layer wetting.

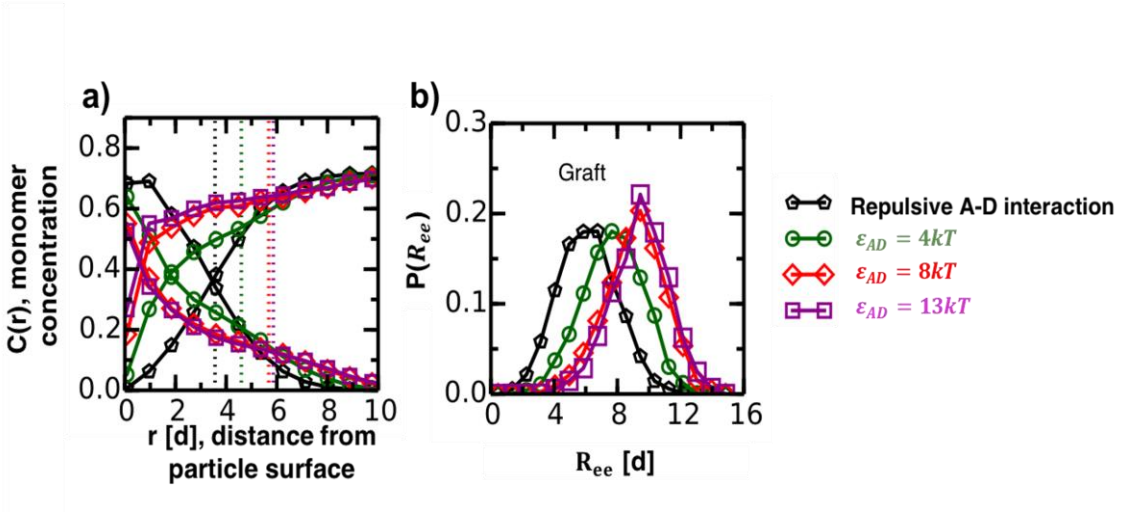

Figure S4. *a) Graft and matrix monomer concentration profiles for PNCs with different strengths of A-D attraction ε_{AD} compared to the case of repulsive A-D interaction (black curve). The grafted brush heights are shown as vertical dotted lines. b) Graft chain conformations for the above cases (as labeled). These results are for PNCs of D=5d, grafting density of 0.65 chains/d^2 and N_G=N_M=20, with every graft and matrix bead containing an acceptor and donor site, respectively.*

D. Impact of directional A-D interaction strength on the distribution of free volume per graft chain

Our results in Figure 6e (D = 5*d*, grafting density of 0.65 chains/d^2 and $N_G = N_M = 20$) show that the free volume per graft chain in case of directional A-D interaction with $\varepsilon_{AD} = 13kT$ is lower than the corresponding free volume in case of PNCs with attractive graft-matrix interaction with $\chi_{GM} = -0.5$ despite the two cases showing equivalent wetting. Since A and D beads are smaller in size relative to G and M beads (i.e., smaller σ in the attractive U_{AD} LJ potential than U_{GM} LJ potential) one may think that interacting A-D beads are held closer together than interacting G-M beads, causing an artificial reduction in free volume per graft chain in the former case. We prove that this is not the case by plotting in Figure S5 the probability distribution of free volume per graft chain for PNCs with $\chi_{GM} = -0.5$ and for PNCs with attractive A-D interaction at different strengths of A-D interaction, $\varepsilon_{AD} = 4kT$, $8kT$, and $13kT$. We find that the free volume per graft chain reduces as the strength of A-D interaction increases from 4-13kT and the free volume for PNCs with an A-D interaction strength of $4kT$ is higher than that for PNCs with $\chi_{GM} = -0.5$. This shows that reduction in free volume in case of PNCs with $\varepsilon_{AD} = 13kT$ is not a manifestation of model implementation because if that were the case it would have led to a lower free volume at all strengths of A-D interaction.

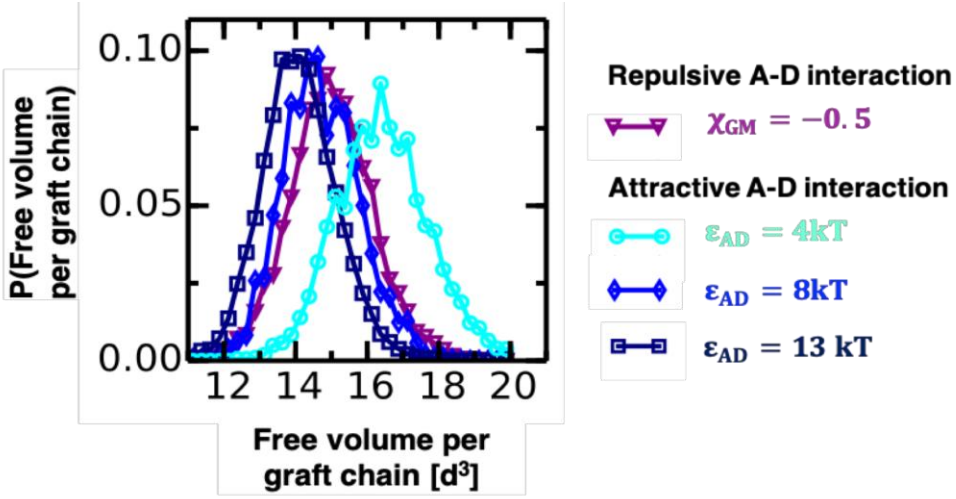

Figure S5. *Probability distribution of free volume per graft chain for four cases: i) PNCs with χ_{GM} = -0.5 and repulsive A-D interaction (magenta curve), PNCs with χ_{GM} = 0 and attractive A-D interaction with ii) $\varepsilon_{AD} = 4kT$ (cyan curve), iii) $\varepsilon_{AD} = 8kT$ (blue curve) ,iv) $\varepsilon_{AD} = 13kT$ (navy curve). These results are for PNCs of D = 5d, grafting density of 0.65 chains/d^2 and N_G=N_M=20, with every graft and matrix bead containing an acceptor and donor site, respectively.*

References

1. Ghobadi, A. F.; Jayaraman, A., Effect of backbone chemistry on hybridization thermodynamics of oligonucleic acids: a coarse-grained molecular dynamics simulation study. *Soft Matter* **2016,** *12*, 2276-2287.

2. Jones, J. E., On the determination of molecular fields.—II. From the equation of state of a gas. *J. Proc. R. Soc. Lond. A* **1924,** *106*, 463-477.
3. Weeks, J. D.; Chandler, D.; Andersen, H. C., Role of repulsive forces in determining the equilibrium structure of simple liquids. *The Journal of chemical physics* **1971,** *54*, 5237-5247.
4. Heo, K.; Miesch, C.; Emrick, T.; Hayward, R. C., Thermally reversible aggregation of gold nanoparticles in polymer nanocomposites through hydrogen bonding. *Nano Letters* **2013,** *13*, 5297-5302.
5. Emsley, J., Very strong hydrogen bonding. *Chemical Society Reviews* **1980,** *9*, 91-124.